Photogrammetry and Kinematic GPS: Results of a High Accuracy Test

Abstract

Aerial triangulation with kinematic GPS support has become an important issue during the past few years. This article reports on the results of a research project that was aimed at demonstrating the valuable contributions that kinematic GPS can make to photogrammetric bundle triangulation. An accuracy of μ_{xy} = 5 cm in planimetry and μ_z = 8 cm in height was obtained for ground check points from an image scale of 1:10,000 with only four control points in the block corners. This accuracy corresponds to the values which can be obtained with a large number of ground control points (bridging distance i = 2b) but without integration of kinematic GPS data. It is argued that in this project the so-called GPS "drift" parameters are cumulative effects of errors in the interior orientation of the metric camera and residual errors from coordinate transformations.

Introduction

Since it has been demonstrated that GPS systems can be used for quasi-kinematic measurements (Remondi, 1985), the scope of surveying applications has increased steadily. One particularly important application arises in photogrammetric block triangulation. The use of kinematic GPS during the photo flight permits the number of ground control points to be substantially reduced, thus rendering the block triangulation more efficient and economical. In a study with synthetic data (Gruen and Runge, 1988), the accuracy potential of a combined GPS/bundle solution was demonstrated and the favorable structure of such a system with respect to the determinability of additional parameters for self-calibration was shown.

In a number of empirical investigations throughout the past seven years or so, various problems with kinematic GPS have surfaced and only a very few projects could claim success.

Our project, "GPS-Supported Aerial Triangulation," whose aim was to verify the theoretical predictions and whose results will be presented here, was started in 1989. It was funded by the Federal Institute of Technology (ETH) Zurich and performed as a cooperative effort of the geodesy and photogrammetry groups of the Institute of Geodesy and Photogrammetry. The data were supposed to be collected over the testfield "Uster" near Zurich, Switzerland, which served as a photogrammetric test field of high accuracy in previous investigations (Gruen, 1986).

After a semi-successful flight in 1990, we had bad luck in 1991 because no suitable GPS window was available throughout this year. However, in March 1992 successful flights on two consecutive days were made covering the full block, both giving good clean GPS data. For a comprehensive report of the complete project, see Gruen *et al.* (1992).

One critical issue in GPS processing is the resolution of carrier wave ambiguities. Gurtner *et al.* (1985) have shown that position accuracies in the sub-centimetre level are possible if the ambiguities can be fixed to integer values. The most stringent conditions for real-time processing have been recently studied in great detail by Frei (1991). The project presented here deals with aerophotogrammetric surveying in the off-line mode. It is, therefore, possible to take advantage of the total data set acquired during the entire flight to estimate the ambiguities.

For our investigations with synthetic data, we could expect an accuracy of μ_{xy} = 5 cm in planimetry and μ_z = 8 cm in height for the ground points (given an image scale of 1:10,000), $\hat{\sigma}_0$ = 5 μm, and a positional accuracy of antenna and projection centers of 10 cm in all three coordinate axes.

It will be shown that these theoretical expectations could be practically confirmed in this project.

Test Configuration and Data Acquisition

The selected test field is the area of Uster near Zurich and is well suited for the purpose (Figure 1). Its nearness to the airport and the existence and high quality of about 100 reference points make it an ideal test field for investigations. This test field has been used in previous photogrammetric block accuracy tests (Gruen, 1986). The geodetic network points are known to have a coordinate accuracy of 5 mm in planimetry and 6 mm in height or better. The 94 points which were used in this test are distributed quite homogeneously over the whole area (Figure 8).

Due to the limited capacity of data storage in the Trimble SST GPS receivers, the photogrammetric block was flown on two consecutive days during the same optimal GPS window, with up to six satellites simultaneously being received. The duration of the flights was about 1½ hours each. To allow differential processing, one receiver was installed on a reference site at the airport and two others were mounted on the airplane (a Twin-Otter). The reference and one of the moving receivers were dual frequency receivers (L1 and L2); the second moving receiver, however, was only an L1 receiver. The dual frequency receivers collected the GPS data at 1 Hz, the L1 receiver at 2 Hz. The data consisted of phase measurements on L1 and L2, C/A-code measurements on L1, and P-code measurements on L2. During the flight the data were only collected and then downloaded, while the processing was done in an off-line mode.

The photogrammetric camera used was a Wild RC20 with a camera constant of 15 cm. Eight strips with a lateral overlap of 60 percent were flown at a height of about 1500 m over ground, resulting in an image scale of 1:10,000. Within

Photogrammetric Engineering & Remote Sensing,
Vol. 59, No. 11, November 1993, pp. 1643–1650.

0099-1112/93/5911–1643$03.00/0

A. Gruen
M. Cocard
H. -G. Kahle
Institut für Geodäsie und Photogrammetrie,
ETH-Hönggerberg, CH-8093 Zürich, Switzerland.

each strip, 19 pictures were taken with an overlap of 80 percent. For processing, only every second photograph was used, resulting in 60 percent forward overlap. Table 1 shows the project specifications.

To connect the GPS results of the antenna coordinates to the coordinates of the projection centers, an accurate knowledge of the time of exposure and the components of the eccentricity vector from the projection center of the camera to the phase center of the antenna is required. The synchronization problem was solved by recording in the GPS receiver the time of an incoming pulse, sent by the camera during the exposure. This pulse was recorded in GPS time by the Trimble receiver and stored in the raw data. The pulse emitted by the camera is off from the correct center time of exposure with an estimated standard deviation of 50 microseconds. Given an airplane velocity of 300 km/h, this amounts to only 4 mm uncertainty in the recording of the antenna position. The eccentricity vector was determined on the ground by terrestrial measurements with theodolite, distance measurements, and leveling. The set of attitude values of the camera was held fixed, defining a camera-related reference frame in which the components of the eccentricity vector were determined. This was done for both antennas with an accuracy at the centimetre level. These two pieces of information, the recording of the exposure time and the determination of the eccentricity vector, permit the GPS results to be connected with the photogrammetric projection centers.

Figure 2 shows the local network for the measurement of the antenna eccentricity vector. Figure 3 indicates the flight pattern and the positions of the perspective centers. Figure 4 shows the height profiles of the flight lines. Obviously, the second day (5 March) gives a less smooth pattern due to harsher wind conditions.

Processing of Kinematic GPS Data

Before processing the flight data, the coordinates of the reference station at the airport were determined by connecting the point to a permanent station in Zimmerwald by GPS. Because the baseline length was about 100 km, it was possible to solve for the L1 and L2 ambiguities and to calculate an ambiguity fixed solution, using the ionosphere-free L3 combination. This procedure permitted the geocentric coordinates of the reference site at the airport to be fixed within an accuracy of a few millimetres with respect to the coordinates of the astronomical observatory in Zimmerwald. These values for the reference station were then introduced as fixed quantities into the processing of the flight data.

For the computation of the kinematic GPS data, an approach using code and phase measurements simultaneously in a differential mode was adopted. The corresponding observation equations of the single difference code measurements are

$$\Delta\rho^i_k = \rho^i_k - \rho^j = d^i_k - d^j + \Delta cl_{jk},$$

and, for the single difference phase measurements,

$$\Delta\phi^i_k = \phi^i_k - \phi^j = d^i_k - d^j + \Delta cl_{jk} + \lambda A^i,$$

where

ρ is the pseudo-range measurement,
ϕ is the phase measurement,
d is the distance between satellite and receiver,
A is the ambiguity related to the phase measurement,
Δcl is the differential synchronization error of the receiver clocks, and
λ is the wavelength of carrier phase.

The superscripts i designate the satellite. The subscripts j

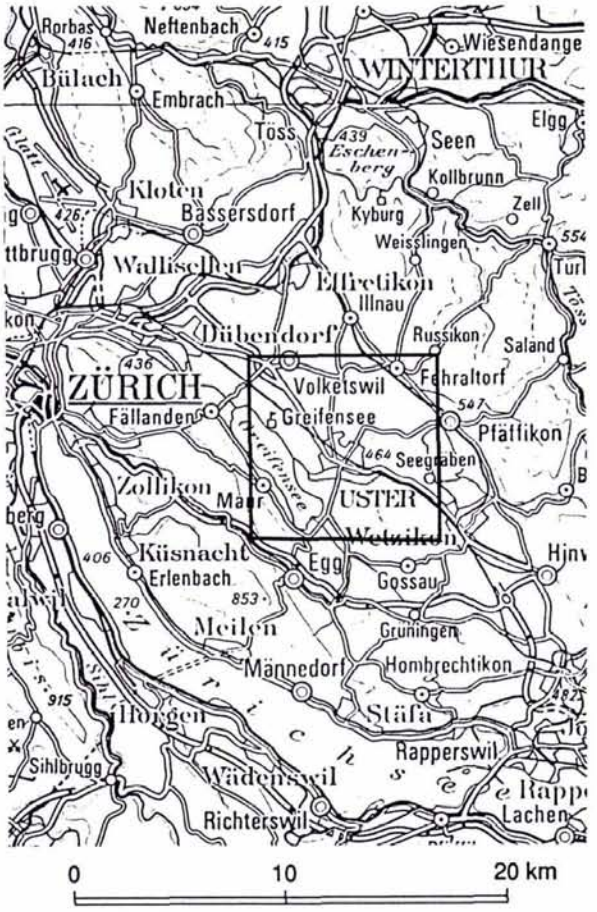

Figure 1. Testfield Uster near Zurich. Courtesy of Swiss Topographical Service (Landestopographie).

TABLE 1. PROJECT SPECIFICATIONS

Test area	Uster, near Zurich (Switzerland)
Size	7.5 by 9.5 km
Mean elevation	500 m
Number of check points	94
Airplane	Twin Otter
Dates of flights	4 March 1992 (5 strips) 5 March 1992 (3 strips)
Flying height over ground	1500m
Duration of flights	about 1.5 hours each
Photogrammetric camera	Wild RC20
Lens	15/4 UAGA-F
Camera constant	152.85 mm
Film	SW/Panatomic X (23 x 23 cm)
Photogrammetric block	
Image scale	1: 10'000
Forward overlap	80% (60% used for processing)
Lateral overlap	60%
Number of strips	8
Flight direction	Equal
Number of exposures	152 (8 strips X 19 per strip)
Number of photographs used	80

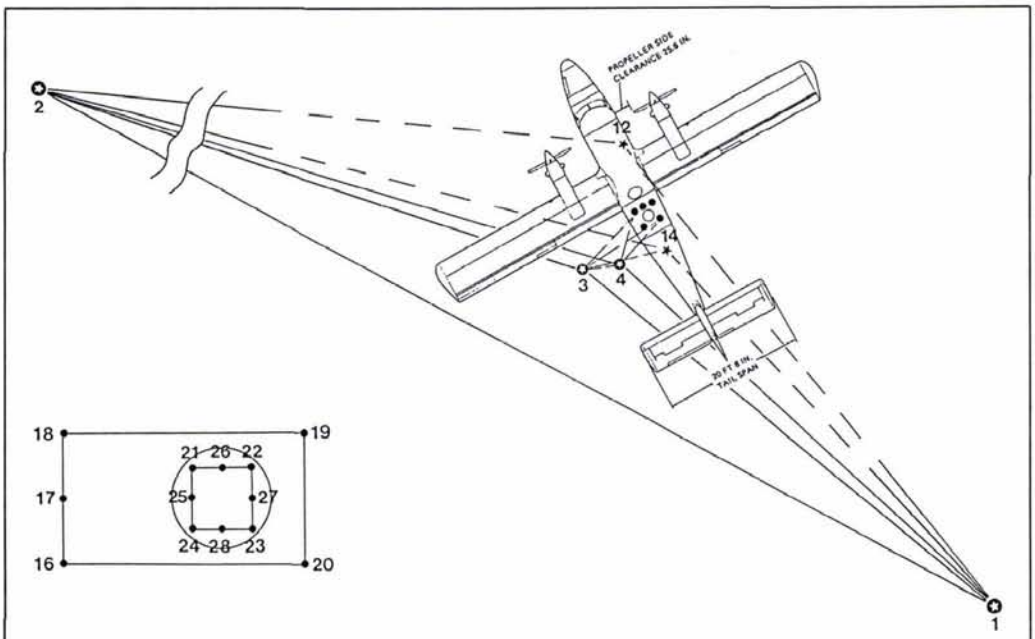

Figure 2. Geodetic determination of the eccentricity vectors of the antennas (Points 12 and 14) related to the camera frame.

and k are related to the reference station and the airplane antenna, respectively. The clock and the position of the satellite, as they are given by the broadcast ephemeris, are supposed to be known and are therefore not included in the observation equations.

An *a priori* accuracy for the measurements is assigned to the phase and code differences. These values may be quite different, depending on the quality of the receiver. Typical values for the *a priori* RMS for different types of observations are

Phase	2 to 5 mm
C/A code	1 to 5 m
P-Code	0.2 to 0.8 m

The processing was performed in two steps.

In a first step, the time-invariant parameters are determined. Parameters which are considered as invariant are the ambiguities and the coordinates at rest before and after the flight. For each epoch, all time-variant parameters are eliminated from the normal equation system, and the reduced normal equation system is accumulated over the total time span. By inversion, one obtains first the floating point solution for the ambiguities and the coordinates. The program then attempts to fix the double difference ambiguities to integers. If this is not possible, the floating point solution can be used. In a second step, the values for the ambiguities obtained from the previous step are then used to calculate the coordinates of the moving receiver for every epoch. The quality of the result strongly depends on the quality of the ambiguity estimation, and the best possible result is obtained when all ambiguities are resolved. Nevertheless, even information from a floating point solution can be used in a photogrammetric bundle block adjustment. Figure 5 shows a schematic representation of the steps involved for the post-processing of kinematic GPS data. The processing software was developed by M. Cocard, Institute of Geodesy and Photogrammetry, ETH Zurich (Cocard, 1993).

Determination and Accuracy of Antenna Coordinates

Figure 6 shows in a schematic overview how the GPS recordings are reduced to a final local horizontal coordinate system in which the bundle adjustment will be performed.

Interpolation of Antenna Coordinates

The position of the antenna obtained by the process described in the previous section refers to the full-second GPS recordings. Because the exact times of the camera exposures have also been recorded by the receiver, it is possible to interpolate the antenna coordinates. For the time being, a simple linear interpolation was chosen. To check the quality and consistency of the coordinates and to get an idea of the error introduced by the linear interpolation, the following investigation was carried out. For every line, the corresponding 1-second data set was reduced to 2-, 4-, 6-, and 8-second data sets. By linearly interpolating the coordinates of the reduced data sets to the middle of the time interval, the interpolated values can be compared to the measured values and a mean square error from the differences can be derived (compare Figure 7).

The exponential function RMS $= a \cdot (1/f)^b$ with the two coefficients a and b, giving the root-mean-square (RMS) error of the interpolation as a function of the data frequency f (in Hz), was then used to fit these values and to predict the mean square error of the interpolation for the 1-second data set. In the following, the mean values over all eight strips are given:

North-South (flight direction) $\quad \text{RMS} = 0.003 \cdot \left(\frac{1}{f}\right)^{1.90}$ [m]

East-West $\quad \text{RMS} = 0.016 \cdot \left(\frac{1}{f}\right)^{1.98}$ [m]

Height $\quad \text{RMS} = 0.018 \cdot \left(\frac{1}{f}\right)^{1.40}$ [m]

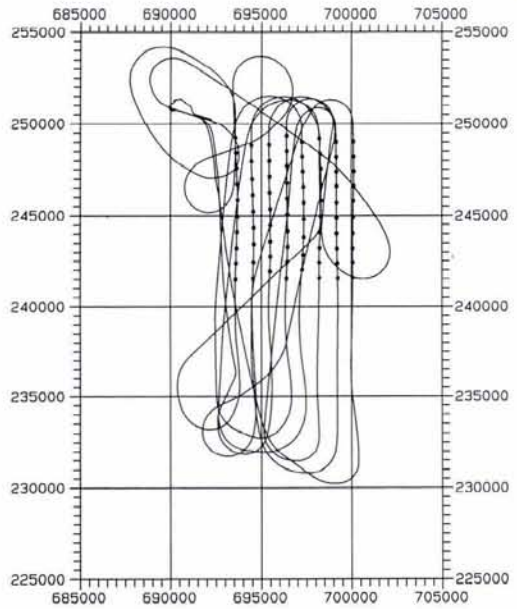

Figure 3. Horizontal track of the two flights (4-5 March 1992) in the Swiss Projection System (units in metres).

Note that, because the interesting frequency is 1 Hz, the corresponding RMS is equivalent to the a coefficient. Thus, the maximum interpolation error amounts to 1.8 cm in the height coordinate.

Coordinate Transformations

The coordinates for the projection centers are given in WGS84 and are connected via the stationary reference receiver at the airport to the coordinates of the permanent station in Zimmerwald (IGS-site). On the other hand, the coordinates of the ground points are given in the Swiss Projection System. To unify the coordinate systems, the coordinates of the ground points are first transformed into their associated geocentric Cartesian system and then shifted to WGS84. Because no WGS84 coordinates of the ground points were available, only three translations were calculated using the point Zimmerwald, where the sets of coordinates were available.

After this unification, all coordinates are available in WGS84, but, for numerical reasons in the bundle adjustment, a predefined six-parameter transformation, consisting of three translations and three rotations, was performed in order to finally have Cartesian coordinates in a local horizontal system.

Comparison of GPS Antenna Coordinates

The 80 photographs of the block were measured on the Wild AC3 Analytical Plotter. Besides the 94 signalized points, 313 natural tie points had to be included. This resulted in a total number of 2020 image points, corresponding to approximately 25 points per photograph. Given a sufficient number of ground control point coordinates, the GPS antenna coordinates can be determined twice: directly from the GPS and indirectly utilizing a photogrammetric bundle triangulation. The latter gives the coordinates of the projection centers, and a correction for the antenna offset results in the antenna coordinates. For this version, the bundle adjustment was performed with all 94 ground control points and 12 additional parameters (Ebner, 1976) for self-calibration.

For the complete block, the RMS values computed from differences GPS − Photogrammetry gave

$$\mu_x^A = 27.2 \text{ cm}, \quad \mu_y^A = 74.6 \text{ cm}, \quad \mu_z^A = 31.5 \text{ cm}.$$

The x coordinate is identical with the flight direction. "A" stands for "antenna."

At a first glance these values render a rather pessimistic picture. Hoewever, after the elimination of block-invariant

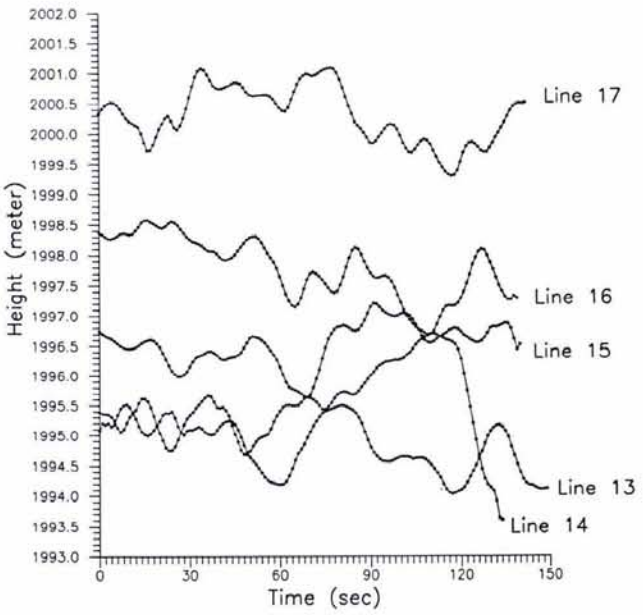

(a)

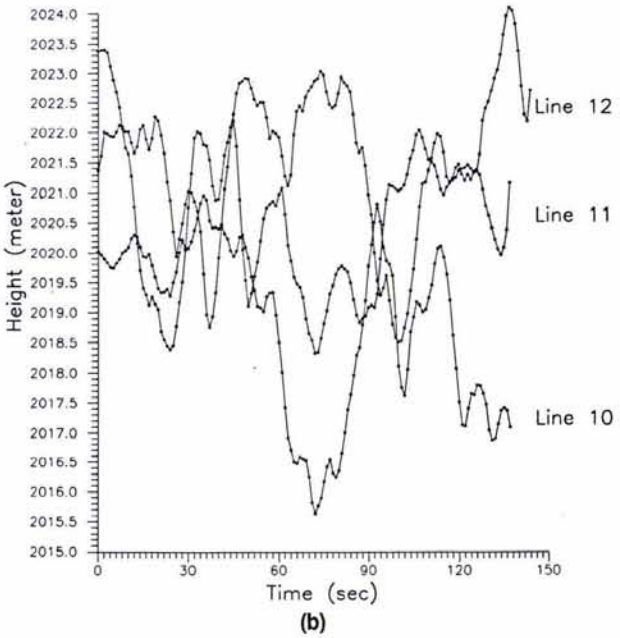

(b)

Figure 4. Height profiles of the photogrammetric strips of (a) first day, (b) second day.

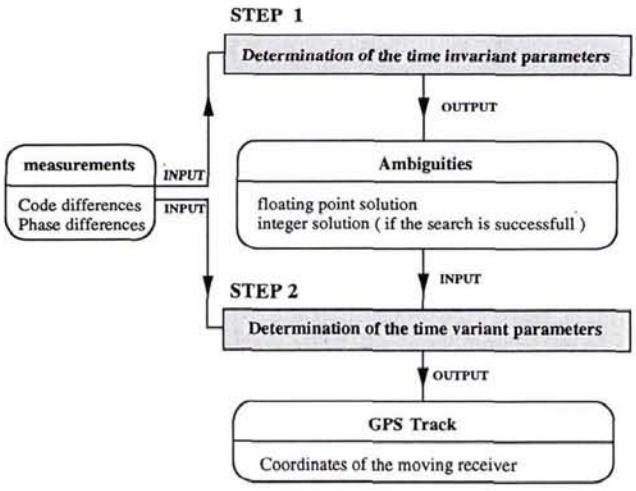

Figure 5. Processing scheme for kinematic GPS data.

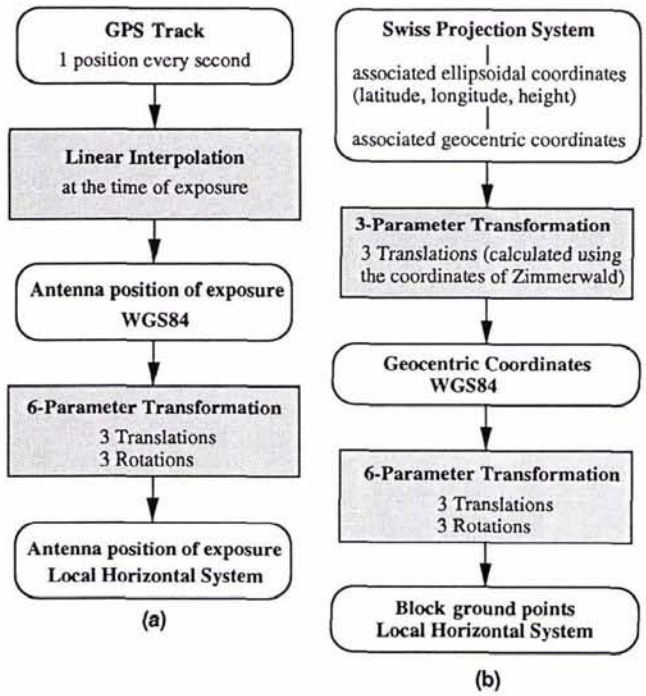

Figure 6. Coordinate transformations. (a) Antenna: GPS Track to Local Horizontal System. (b) Block Ground Points: Swiss Projection System to Local Horizontal System.

shift parameters Δx, Δy, Δz, we obtain:

$$\mu_x^A(sc) = 12.7 \text{ cm}, \quad \mu_y^A(sc) = 17.4 \text{ cm}, \quad \mu_z^A(sc) = 7.5 \text{ cm}$$

where *sc* indicates "shift corrected."

Even better values can be achieved if the shift parameters are computed as strip-invariant. This version is not shown here because, as it turned out later, it did not improve the ground check point coordinates.

But even these values do not compare well with the theoretical standard deviations computed from the inversion of the normal equations.

Standard deviations of the projection center coordinates from the bundle adjustment were

$$\sigma_{xy}^A = 7.4 \text{ cm}, \quad \sigma_z^A = 3.6 \text{ cm}.$$

This significant discrepancy between theoretical and empirical values for the projection center coordinates has been observed in other projects in the past and has given rise to a variety of speculations. In most cases a GPS "drift" is identified as the major source for these deviations.

If ambiguities are not a problem (as is the case in our project), a drift can only result in L1 processing through ionospheric effects. This would result in a scale factor of less than 5 ppm and amount to a maximal offset of 5 cm throughout the test field area. Therefore, this effect cannot explain the much larger deviations observed here.

Instead of assuming a GPS drift, we suspect two other error souces. First, there are transformation discrepancies going from WGS 84 (GPS antenna coordinates) to the Swiss Projection System (ground points) or vice versa. There were no identical GPS/Swiss Projection System points in the block. Second, any errors in the interior orientation elements (principal point coordinates and camera constant) will cause, in the event of flat terrain, shifts Δx, Δy, Δz in all three coordinates of the projection centers of the bundle adjustment. If the projection centers are fixed by GPS observations (see the next section), this effect will be compensated by the constant terms of the "drift parameters." Therefore, the constant portion of the drift parameters and the effects of the interior orientation parameters cannot be separated under our test conditions (equal strip directions). Here it should be noted that the separation capability depends on the pattern of flight directions and on the introduction of the shift parameters as either block- or strip-invariant. Coordinate transformation errors are block-invariant, whereas errors of interior orientation and possible GPS drift errors depend in sign on the flight direction.

Results of Controlled Bundle Adjustment

A truly conclusive system test must include ground check points, because the determination of ground point coordinates is the ultimate aim of blocktriangulation.

Figure 8 shows the block layout, including projection centers and control points.

In the subsequent investigations, the following system parameters will be varied:

- Number of control points: 94, 29, 5, 4.
- Drift parameters: Constant, constant + linear; one set for the whole block (block-invariant-1 set); one set separately for

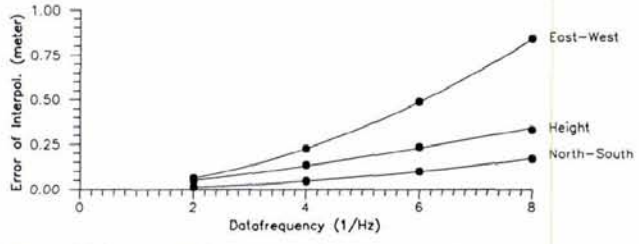

Figure 7. Interpolation errors of antenna trajectories.

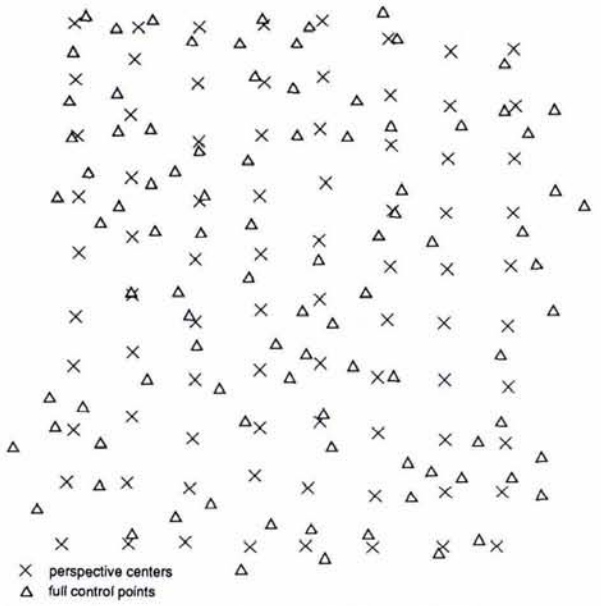

Figure 8. Block layout of GPS-block "Uster 92."

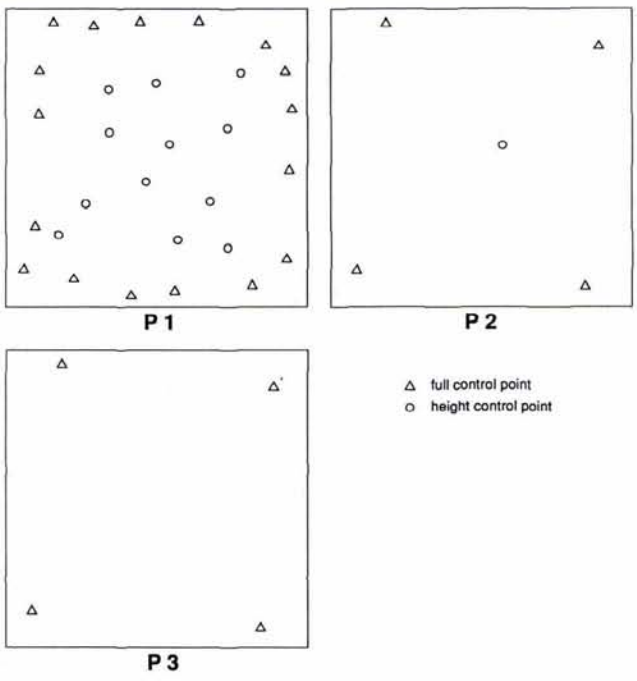

Figure 9. Control point versions for GPS-block "Uster 92."

each day of flight (flight-invariant-2 sets); one set for each strip (strip-invariant-8 sets).

Figure 9 shows the different control point versions. They are marked **P1, P2, P3. P1** corresponds to a bridging distance $i = 2b$ for the control points. **P0** is the version with full (94) control points and no check points. In all versions, 12 additional parameters have been used for self-calibration and all of them were well determinable.

The versions without GPS data were computed with the bundle program BUND of the Institute of Geodesy and Photogrammetry, ETH Zurich, while the bundle versions with GPS data were generated with the program ACX of the Institut Cartogràfic de Catalunya, Barcelona (Colomina, 1989).

As a first important result, it was obvious that the versions with full drift parameter sets (constant + linear terms) did not improve the empirical accuracy values. Therefore, these versions are not presented here. Table 3 shows the results of all computations with reduced drift parameter sets (*only constant terms*). *Considering the arguments presented* in the section on Comparison of GPS Antenna Coordinates, these parameter sets will now be called "pc-offsets" (projection center offsets). These pc-offsets are marked as follows:

1 . . . Block-invariant
2 . . . Flight-invariant
8 . . . Strip-invariant

With $\hat{\sigma}_0 = 4.6$ µm without GPS data, the overall accuracy level is not extremely high due to the fact that only 30 percent of all object points are signalized and thus clearly marked. Through the additional GPS data constraints, the level for $\hat{\sigma}_0$ rises to 4.8 to 5.2 µm.

This points towards an inappropriate stochastic modeling of the GPS antenna observations. In fact, the *a priori* chosen standard deviation of 3 cm for both planimetric and height coordinates turned out to be too optimistic. Therefore, too much constraint was executed regarding these observations, leading to a deterioration of $\hat{\sigma}_0$.

It is evident that the use of separate pc-offsets for all strips (version 8) deteriorates the results in case of sparse control point distribution (**P2, P3**) both in theory and in practice. The modeling with two sets (one per flight) neither deteriorates nor improves the results significantly. Therefore, it is sufficient to use just one set for the whole block. Even with very sparse control distribution (**P3**, four full control points in the block corners), a very good accuracy can be reached ($\mu_{xy} = 5.2$ µm, $\mu_z = 8.7$ µm at the photo scale) if GPS data are integrated. These values are in good correspondence with the theoretical ones ($\sigma_{xy} = 4.5$ µm, $\sigma_z = 8.0$ µm) and equivalent to those which can be reached with dense control distribution (**P1**, $i = 2b$) but without GPS data ($\mu_{xy} = 5.0$, $\mu_z = 8.2$ µm).

Conclusions

If ambiguities in kinematic GPS processing can be resolved, and if ionospheric effects on the L1 processing can be neglected in a relatively small test area or if L3 is used for processing, then "drift" effects should not be expected. However, residual errors in the camera's interior orientation and inaccuracies of the coordinate transformation WGS84 to the

TABLE 2. RECEIVER CHARACTERISTICS

GPS-receivers	Employment	Meas. Freq.	Code-meas.	Phase-meas.
1. Trimble Surveyor II	stationary	1 Hz	C/A P	L1 L2
2. Trimble Geodesist	on the airplane	1 Hz	C/A P	L1 L2
3. Trimble Aerial	on the airplane	2 Hz	C/A	L1

TABLE 3. RESULTS OF BUNDLE BLOCK ADJUSTMENTS "USTER 92"

Control point version	PC-offsets	$\hat{\sigma}_0$ [μm]	μ_{xy} [μm]	μ_z [μm]	σ^*_{xy}) [μm]	σ^*_z) [μm]	No. control points plan.	No. control points height	No. check points plan.	No. check points height
	1	5.2	–	–	3.5	6.6	94	94	–	–
	2	5.1	–	–	3.6	6.5	94	94	–	–
P0	8	5.0	–	–	3.5	6.5	94	94	–	–
	Without GPS	*4.8*	–	–	*4.0*	*7.6*	94	94	–	–
	1	5.0	4.5	8.8	3.8	6.9	17	29	77	65
	2	4.9	4.4	7.9	3.8	6.9	17	29	77	65
P1	8	4.8	4.2	8.3	3.8	6.9	17	29	77	65
	Without GPS	*4.6*	***5.0***	***8.2***	***3.9***	***7.3***	17	29	77	65
	1	4.9	5.3	9.0	4.5	7.7	4	5	90	89
	2	4.9	5.2	8.8	4.5	7.7	4	5	90	89
P2	8	4.8	5.6	13.3	4.7	8.8	4	5	90	89
	Without GPS	*4.6*	*14.3*	*23.7*	*5.7*	*12.2*	4	5	90	89
	1	4.9	**5.2**	**8.7**	**4.5**	**8.0**	4	4	90	90
	2	4.9	5.0	8.3	4.5	8.1	4	4	90	90
P3	8	4.8	6.9	47.9	4.7	12.4	4	4	90	90
	Without GPS	*4.4*	*12.5*	*177.0*	*5.6*	*18.3*	4	4	90	90

μ_{xy}, μ_z are empirical accuracy values from check point residuals in planimetry and height (values given at photo scale)
σ_{xy}, σ_z are theoretical precision values from the inversion of the normal equations in planimetry and height (values given at photo scale)
* The numbers for σ_{xy} and σ_z refer to all new points of the system, including non-signalized tie points

national projection system (in case not enough common points are used) require that constant projection center offset parameters (pc-offsets) be included in the hybrid bundle solution. This project has shown that, if only one camera is used, just *one* set of three parameters for the whole block is sufficient. This, in turn, does not require a non-standard block structure, as for instance cross-strips at the block perimeter or extra control point chains. In our project we could show that the use of four control points in the block corners results in the same accuracy values (μ_{xy} = 5.2 μm, μ_z = 8.7 μm, $\hat{\sigma}_0$ = 4.9 μm) as if a dense control point distribution (i = 2b) would be used without GPS data. Notwithstanding the need for further practical testing under a variety of different conditions, our results give a very optimistic outlook for future projects. It is our experience that the theoretical potential of kinematic GPS can practically be fulfilled in the context of photogrammetric block adjustment. It is now up to the system manufacturers to provide combined camera/GPS systems and processing software that can match the customers' expectations and needs.

Acknowledgments

This is to thank all persons involved in the project for their valuable contributions. R. Huebscher, the camera operator, and the Swiss Cadastral Authority (Vermessungsdirektion) provided for the aircraft and camera and were always very responsive to our requests. I. Colomina generously gave us access to his hybrid bundle program ACX and was readily available for advice. Z. Parsic undertook the tedious work of image coordinate measurements. We are indebted to Dr. A. Geiger, who offered helpful suggestions and practical advice during all stages of the project. Our special thanks go to him for his persistent help in the set-up of the GPS campaign. We are most grateful to Dr. G. Forlani and B. Moser for their work on the photogrammetric part of the active project. The funding of this project by ETH Zurich is also acknowledged.

References

Ackermann, F., 1992. Operational rules and accuracy models for GPS-aerotriangulation. *Int. Archives of Photogrammetry and Remote Sensing*, 29(B3):691–700.

Cocard, M., 1990. Kinematic experiences with GPS and laser tracker. *Cahiers du Center Européen de Géodynamique et de Séismologie: GPS for Geodesy and Geodynamics*, pp. 19–25.

———, 1993. *High Precision GPS Processing in Kinematic Mode.* Dissertation under preparation, ETH Zurich.

Cocard, M., and A. Geiger, 1992. Systematic search for all possible wide lanes. *Proceedings of the 6th International Geodetic Symposium on Satellite Positioning*, Columbus, Ohio, pp. 312–318.

Cocard, M., A. Geiger, H.-G. Kahle, G. Forlani, A. Grün, and B. Moser, 1991. *GPS-Supported Photogrammetric Triangulation* (in German). Second Intermediate Report of ETH research project, Zurich.

Colomina, I., 1989. Combined adjustment of photogrammetric and GPS-data. *Schriftenreihe des Instituts für Photogrammetrie*, Universität Stuttgart, 13:313–328.

Danuser, G., U. Schor, L. Bagnaschi, M. Cocard, and A. Geiger, 1992. *Ableitung kinematischer Grössen aus GPS-Messungen.* IGP-Bericht 201, ETH Zurich.

Ebner, H., 1976. Self calibrating block adjustment. *Int. Archives of Photogrammetry*, Vol. 21, Part 3, Helsinki.

Forlani, G., 1990. *GPS-Supported Photogrammetric Triangulation.* First Intermediate Report of ETH research project, Zurich.

Frei, E., 1991. *Rapid Differential Positioning with the Global Positioning System (GPS).* Geodätisch-geophysikalische Arbeiten in der Schweiz (Swiss Geodetic Commission).

Gruen, A., 1986. Project "Uster" – ein Beispiel moderner photogrammetischer Punktbestimmung. *Vermessung, Photogrammetrie, Kulturtechnik*, (4):187–191.

Gruen, A., and A. Runge, 1988. The accuracy potential of self-calibrating aerial triangulation without control. *Int. Archives of Photogrammetry and Remote Sensing*, Vol. 27, Part B3, Kyoto.

Gruen, A., B. Moser, H.-G. Kahle, M. Cocard, and A. Geiger, 1992. *GPS-Supported Photogrammetric Triangulation* (in German). Final Report of ETH research project, Zurich.

Gurtner, W., G. Beutler, I. Bauersima, and T. Schildknecht, 1985.

Evaluation of GPS carrier difference observations: The Bernese second generation software. *Proceedings of the First International Symposium on Precise Positioning with the Global Positioning System*, Rockville, pp. 363–372.

Remondi, B.W., 1985. Global Positioning System carrier phase: Description and use. *Bulletin Geodesique*, 59:361–377.

Call for Papers

9TH ANNUAL GEOGRAPHIC INFORMATION SYSTEMS ISSUE

Photogrammetric Engineering & Remote Sensing

The American Society for Photogrammetry and Remote Sensing will publish its Ninth Annual Geographic Information Systems issue of *PE&RS* in November 1994. Special Guest Editors are Ann Maclean of the Michigan Technological University and Gordon Maclean of Maclean Consultants, Ltd. This issue will contain both invited and contributed articles.

Authors are especially encouraged so submit manuscripts on the following types:

- Spatial modeling of natural resources
- Assessing spatial accuracy of GIS information
- Use of GIS in remote sensing activities
- Economic issues of GIS utilization by local and county governments
- Applications of digital orthoimagery in GIS
- Integration of GIS and decision support systems
- Use of GPS in GIS

All manuscripts, invited and contributed will be peer-reviewed in accordance with established ASPRS policy for publication in *PE&RS*. Authors who wish to contribute papers for this special issue are invited to mail five copies of their manuscript to:

Dr. Ann Maclean
School of Forestry and Wood Products
Michigan Technological University
1400 Townsend Drive.
Houghton, MI 49931-1295
906-487-2030; fax 906-487-2915

Dr. Gordon A. Maclean
Maclean Consultants, Ltd.
P.O. Box 655
Houghton, MI 49931-0566
906-482-9692

All papers should conform to the submission standards in "Instructions to Authors" which appears monthly in *PE&RS*. **Manuscripts must be received by 1 February 1994 in order to be considered for publication in this special issue.**